

Breastfeeding promotes early neonatal regulatory T cell expansion and immune tolerance of non-inherited maternal antigens

Hannah Wood¹, Animesh Acharjee¹, Hayden Pearce¹, Mohammed Quraishi¹, Richard Powell¹, Amanda Rossiter¹, Andrew Beggs¹, Andrew Ewer¹, Paul Moss¹, and Gergely Toldi¹

¹University of Birmingham

October 6, 2020

Abstract

Background: Breastfeeding is associated with long-term health benefits, such as a lower incidence of allergy, asthma, diabetes or celiac disease. However, little is known regarding how the maternal and neonatal immune systems interact after parturition when the neonate receives nutrition from maternal breastmilk. **Methods:** We undertook a comparative analysis of immune repertoire and function at birth and 3 weeks of age in a cohort of 38 term neonates born by caesarean section grouped according to feeding method (breastmilk versus formula). We used flow cytometry to study the immune phenotype in neonatal and maternal blood samples and mixed lymphocyte reactions to establish the proliferation response of neonatal versus maternal lymphocytes and vice versa. The microbiome of neonatal stool samples was also investigated using 16S rRNA sequencing. **Results:** We show that the proportion of regulatory T cells (Tregs) increases in this period and is nearly two-fold higher in exclusively breastfed neonates compared to those who received formula milk only. Moreover, breastfed neonates show a specific and Treg-dependent reduction in proliferative T cell responses to non-inherited maternal antigens (NIMA), associated with a reduction in inflammatory cytokine production. **Conclusions:** These data indicate that exposure of the neonate to maternal cells through breastfeeding acts to drive the maturation of Tregs and ‘tolerizes’ the neonate towards NIMA.

Keywords

breastfeeding, microbiome, neonate, non-inherited maternal antigen, regulatory T cell, Th17

INTRODUCTION

Exposure and adaptation to extra-uterine life represents a substantial challenge for homeostatic physiological systems of neonates. Paramount amongst these are modifications within immune function which must facilitate acquisition of a symbiotic microbiome whilst protecting against pathogen challenge. Infection is a significant cause of morbidity and mortality in neonates¹⁻³ but current understanding of the functional capacity of the neonatal immune system in the first few weeks of life remains limited. Substantial differences are observed between neonatal and adult immune function. CXCL8 (IL-8) is the major effector chemokine of neonatal T cells whilst production of IFN- γ is markedly suppressed and a reduction in NK cell numbers is observed⁴.

Elegant multi-dimensional analyses have revealed that profound changes in immune cell numbers, phenotype and proteome are observed within the first week of life and presage initiation of a stereotypic differentiation pathway. This profile is seen in both preterm and term infants and as such appears to represent a response to multiple environmental cues, predominantly microbial, that are received after birth⁵. Dynamic alterations in the interferon and complement pathways, as well as neutrophil-associated signaling, are particularly prominent⁶. However, less is known regarding neonatal immune function and the potential impact of nutritional intake on immune homeostasis.

An important consideration in relation to neonatal immune function is the relative setpoint of immune regulation in the early postnatal period. A range of factors act to limit alloreactive immune responses during pregnancy and avoid immunological rejection of the fetus. This includes an increase in both maternal and fetal-derived regulatory T cells (Tregs)^{7,8} together with preferential differentiation of fetal CD4+ cells towards Treg phenotype⁹ mediated through increased ‘tolerogenic’ dendritic cell activity¹⁰. It is likely that this balance towards relative immune suppression continues into neonatal life but the profile of this, and its relative dependence on the postnatal environment, remain unclear.

The perinatal establishment of the gut microbiome is likely to be a dominant regulator of neonatal immune development. Indeed, colonization with specific commensal bacteria can enhance the development of Treg responses¹¹, whilst dysbiosis disturbs stereotypic immune development and promotes T cell activation⁵. Vertical transmission of maternal microbiota is the initial, and potentially most important, determinant of the neonatal microbiome. In this regard it is notable that the mode of delivery is a critical factor and its influence on childhood microbiome extends for at least 7 years¹². The influence of microbiome composition on long term health outcomes is an area of considerable interest and atypical colonization has been associated with a range of conditions including impaired immune function and increased risk of allergy¹³.

The importance of nutrition as a determinant of the profile of neonatal immunity has been poorly investigated. The natural nutrition for neonates is from breastmilk which contains a range of complex nutrients as well as antimicrobial proteins. Breastmilk also contains bacteria and maternal cells, and as such it is not surprising that exposure to either breastmilk or formula milk significantly influences the composition of the gut microbiome¹⁴.

Differential microbiome composition is likely to act as an indirect influence on how nutrition can modify the neonatal immune profile but there may also be a direct effect from exposure to maternal cells and antigenic proteins within milk. We analyzed how immune phenotype and function evolve between birth and 3 weeks of age in a cohort of healthy neonates born by caesarean section. Our aim was to determine prospective changes in the neonatal adaptive immune response in relation to source of nutrition and neonatal gut microbiome with a specific focus on regulatory T cells.

METHODS

A total of 38 healthy pregnant women who were planned to deliver electively at gestational term by caesarean section were sampled in our study at Birmingham Women’s Hospital, UK. Peripheral blood samples were collected prior to the caesarean section and all women were not in labor and had intact membranes. Cord blood samples were taken immediately after delivery. A peripheral blood sample (up to 2 mL) was taken from the neonate at 3 weeks of age. In addition to the blood samples, a neonatal stool sample was collected at birth and at 3 weeks of age from 29 of the recruited neonates. Exclusion criteria included multiple pregnancy, sepsis risk factors (especially maternal fever or chorioamnionitis), GBS positivity in the current pregnancy, genetic conditions of the fetus or the mother, maternal HIV, maternal TB, maternal new-onset viral infection, maternal hypertensive disorder, maternal endocrine condition or diabetes, maternal asthma and maternal autoimmune conditions, as well as maternal medication other than pregnancy supplements. Peripheral blood samples were also collected from 13 healthy, non-pregnant adults (male/female: 6/7).

Informed written consent was obtained from all pregnant women. The study was reviewed and approved by the East Midlands – Nottingham 2 NHS Research Ethics Committee (reference 16/EM/0379).

Mononuclear cell isolation from blood samples

Blood samples were collected into anticoagulated tubes. Mononuclear cells were isolated by density centrifugation using Lymphoprep (Stemcell Technologies, Seattle, WA, USA). PBMCs were washed with RPMI-1640 medium (Sigma-Aldrich, St. Louis, MO, USA) and used either directly or cryopreserved in fetal bovine serum containing 10% DMSO (Sigma-Aldrich). After thawing, cells were washed with RPMI and re-suspended in enriched media.

Immunophenotyping

Mononuclear cells were prepared as described above for two immunophenotyping panels. Panel 1 was designed to study intracellular cytokine production following stimulation. Cells were stained with FITC-conjugated CD107a (Biolegend, San Diego, CA, USA) at the time of stimulation. Stimulation was performed with phorbol myristate acetate (PMA, 50 ng/mL, Sigma-Aldrich) and ionomycin (1 μ g/mL, Sigma-Aldrich) for a total of 3.5 hours at 37 degrees centigrade. After 30 minutes, 1.25 μ g/mL of monensin (Sigma-Aldrich) was added to stimulated cells for the remaining 3 hours. Cells were then washed with phosphate-buffered saline (PBS, Sigma-Aldrich) and re-suspended. Cell surface staining was performed for 30 minutes on ice in the dark as follows: BV510-conjugated CD4, PerCP-Cy5.5-conjugated CD8, ECD-conjugated CD14/CD19/CD56, APC-Cy7-conjugated CD3 (all from Biolegend) and Live/Dead (red, 488nm, Invitrogen, Carlsbad, CA, USA). After washing, cells were fixed with fixation/permeabilization solution (eBioscience, San Diego, CA, USA) for 30 minutes at room temperature in the dark. Cells were washed with permeabilization buffer (eBioscience). Following centrifugation and re-suspension, the following intracellular dyes were added for 30 minutes at room temperature in the dark: PE-Cy7-conjugated IL-6, AF700-conjugated IFN- γ , AF647-conjugated IL-4, BV421-conjugated IL-17A and PE-conjugated IL-8 (all from Biolegend). Cells were then washed and run on an LSRII flow cytometer equipped with blue, red and violet lasers (BD Biosciences, San Jose, CA, USA). The staining procedure was identical for unstimulated cells. At least 50,000 cells were recorded per sample.

Panel 2 assessed the immunophenotype of cells without mitogenic stimulation. Cells were surface stained with PE-Cy7-conjugated HLA-DR, BV510-conjugated CD4, PerCP-conjugated CD69, ECD-conjugated CD14/CD19/CD56, AF700-conjugated CD45RA, APC-Cy7-conjugated CD3, BV421-conjugated CD25, BV605-conjugated CD31 (all from Biolegend) and Live/Dead (red, 488nm, Invitrogen). After washing, cells were fixed with fixation/permeabilization solution (eBioscience) for 30 minutes at room temperature in the dark. Cells were washed with permeabilization buffer (eBioscience). Following centrifugation and re-suspension, AF647-conjugated FoxP3 (Biolegend) antibodies were added for 30 minutes in the dark. Cells were then washed and run on an LSRII flow cytometer equipped with blue, red and violet lasers (BD Biosciences). At least 50,000 cells were recorded per sample.

In both panels during the gating process, doublets were first excluded based on FSC-A and FSC-H characteristics. Lymphocytes were then identified based on FSC-A and SSC-A characteristics. Dead, as well as CD14+, CD19+ and CD56+ cells were excluded based on positivity in the ECD channel. Further gating was performed within CD3+ cells. Flow cytometry data was analyzed using the FlowJo software package.

T cell proliferation using mixed lymphocyte reaction assay

Mononuclear cells were prepared as described above. Stimulator cells were extracted and re-suspended in enriched media for irradiation. Cells were irradiated at 3000 rad. For responder cells, T cell enrichment was performed using the Easy Sep T cell enrichment antibody mix (1 μ L per 10^6 cells), magnetic beads and Easy Sep Purple Magnet separation (Stemcell Technologies). MLRs were applied in the following combinations: maternal T cell responders vs irradiated cord blood cells, cord blood T cell responders vs irradiated maternal cells, maternal T cell responders vs irradiated neonatal cells and neonatal T cell responders vs irradiated maternal cells. For the setup of neonatal MLRs, all corresponding maternal cells had undergone prior cryopreservation and were thawed as described above. In selected maternal, cord blood and neonatal samples ($n = 6$ each), the T cell enriched suspensions were split between non-CD25-depleted and CD25-depleted samples. Suspensions that were retained for CD25-depletion were depleted using CD25 MicroBeads with magnetic MACS microcolumn separation (Miltenyi Biotec, Bergisch Gladbach, Germany).

To trace proliferation of responder T cells in the assay, 1 μ L of CellTrace Violet dye (Invitrogen) was added per 10^6 cells and incubated at 37 degrees for 20 minutes. 2×10^5 irradiated stimulator mononuclear cells were added at a 2:1 ratio to each responder sample of 1×10^5 in a 96-well round-bottom plate in enriched media. Each sample was run in duplicate. Positive control samples were established with the addition of 5 μ L of CD3/CD28 activator Dynabeads (Thermo Fisher Scientific, Waltham, MA, USA) instead of stimulator cells. Negative controls were established in enriched media only. To each sample and positive control, 10 U of IL-2 cytokine was added. Samples were incubated for 5 days. At day 3, 150 μ L of media per well was replaced

with fresh media. Each sample was harvested and washed with PBS (Sigma Aldrich). Surface staining was performed using APC-Cy7-conjugated CD3, BV510-conjugated CD4 and PerCP-Cy5.5-conjugated CD8 (all from Biolegend). Samples were washed and then re-suspended. 1 μ L of propidium iodide (Biolegend) was added for live/dead discrimination to each sample immediately before flow cytometry was performed on an LSRII flow cytometer equipped with blue, red and violet lasers (BD Biosciences). At least 20,000 cells were recorded per sample.

During the gating process, doublets were first excluded based on FSC-A and FSC-H characteristics. Lymphocytes were then identified based on FSC-A and SSC-A characteristics. Dead cells were excluded based on positivity in the ECD channel. Further gating was performed within CD3+ cells. Flow cytometry data was analyzed using the FlowJo software package.

Cytokine production

MLRs were applied in the combinations as described above. On day 5, supernatants from each well (100 μ L) of selected samples ($n = 13$) were collected and frozen. The concentration of cytokines in each supernatant sample was analyzed in batches after thawing using a custom designed Luminex plate as per the manufacturer's instructions (Bio-Techne, Minneapolis, MI, USA). The concentration of IFN- γ , IL-4, IL-6, IL-8, IL-10, IL-17 and TNF- α were analyzed using a Bio-Plex 200 plate reader and the Bio-Plex Manager 6.1 software (Bio-Rad, Hercules, CA, USA).

Stool DNA extraction, amplification and sequencing

Neonatal stool collection

Whole nappies were removed by the parents and placed into a transport bag. Samples were then taken from the nappies by a gloved study personnel using a sterile scoop and then placed into sterile glass containers. Stool samples were frozen immediately and stored at -20 degrees until DNA extraction.

Extraction of neonatal stool DNA

DNA was extracted from thawed stool samples using the QIAamp Fast DNA Stool Mini Kit (Qiagen, Hilden, Germany). For all extractions 290-310 mg of stool was transferred into Lysing Matrix E 2mL tubes (MP Biomedicals, Illkirch-Graffenstaden, France). Tubes without stool were used as negative controls for each batch of samples. Samples underwent 4 cycles of bead beating for 30 seconds using the FastPrep-24 5G Instrument (MP Biomedicals). The suspensions were heated to 95 degrees for 5 minutes and then centrifuged (2 minutes, 12000 rpm). The remaining extraction steps were performed according to the manufacturer's instructions. DNA was eluted using 100 μ L of elution buffer and samples were centrifuged for 2 minutes to elute the DNA. DNA yield was assessed using the Qubit dsDNA HS Assay kit with a Qubit 2.0 fluorometer (Invitrogen). Extracted DNA was stored at -80 degrees until amplified.

Amplification of bacterial DNA

16S rRNA genes were amplified with primers targeting the V4 region using the standardized Earth Microbiome 16S Illumina Amplicon protocol¹⁵. Samples were processed in batches with appropriate negative controls to ensure there were no contaminants arising from the DNA extraction kits as described earlier¹⁶. Following clean up, the amplicon fragment lengths were assessed for quality using TapeStation (Agilent, Santa Clara, CA, USA). DNA was quantified for each amplicon using the Qubit dsDNA HS Assay kit with a Qubit 4.0 fluorometer (Invitrogen). Each DNA library was normalized to a DNA concentration of 4 nM and then pooled to contain 5 μ L DNA from each sample. The quality of the pooled DNA sample was assessed on TapeStation and demonstrated an average base pair length of 401 bp. Using the Qubit method described above, the pooled DNA was quantified to an average 1.61 ng/ μ L.

Sequencing and Identification of bacterial DNA

The pool of stool DNA was sequenced in one sequencing run. Sequences were obtained using an Illumina MiSeq paired-end 250-bp protocol for 500 cycles. The PCR was performed in one batch with appropriate

negative controls following which paired-end sequencing (2×250bp) was performed on the Illumina MiSeq platform (Illumina, San Diego, CA, US) and processed using the Quantitative Insights Into Microbial Ecology 2 (QIIME2) pipeline¹⁷. Samples were rarefied prior to alpha and beta diversity analysis. Taxonomy assignment was done against the Silva-132-99% OTUs database and differences in relative abundance of taxa between cohorts were analyzed using linear discriminant analysis (LDA) effect size (LEfSe). Taxa with LDA > 2 at a p value < 0.05 were considered significant.

Univariate statistical modelling

Statistical analysis

Comparisons were made using the Kruskal-Wallis test or the Mann-Whitney U test as the distribution of data appeared to be non-normal according to the Shapiro-Wilk test. p values < 0.05 were considered significant. Data are presented as median [interquartile range]. Statistics were calculated using the GraphPad Prism 5 and 8 software.

Random Forest machine learning method

We used Random Forest (RF) for data integration and individual data set analysis. RF is a machine learning ensemble method in conjunction with multiple learning algorithms to obtain better predictive performance¹⁸. RF can be used for both classification and regression. In our analysis we used RF for classification using the feeding method (exclusively breastfed vs exclusively formula-fed) as outcome variable and treating each of the data sets separately. We used ntree = 500 and mtry = square root of variables in our models. We used two packages for RF analysis (randomForest and varSelRF) in R (v3.6.1).

The Backward elimination method

To select features automatically we iteratively fitted random forests, at each iteration building a new forest after discarding 20% of the features with the smallest variable importance. The selected set of features was used as a predictor to fit the model to check the ‘out of bag’ (OOB) error rate. We examined the OOB error rates from all fitted random forests. We chose the solution with the smallest number of variables whose error rate was within one standard error. This procedure was performed iteratively using the varSelRF package in R (v3.6.1).

Network analysis

We used the qqgraph package in R (v3.6.1) to perform network analysis. A network is a set of nodes and a set of edges, where each node represents either an immune parameter or an operational taxonomic unit (OTU) from microbiome analysis whereas the edges represent associations amongst them. Pearson correlation coefficients were used to quantify the strength of associations between combinations of immune parameters or OTUs.

RESULTS

Neonates develop both protective and tolerogenic adaptive immune responses in the first three weeks of life

Thirty-eight healthy mother-and-baby dyads were sampled in our study and all deliveries were performed by caesarean section (male/female: 17/21, gestational age: 39 [39-39] weeks, birth weight: 3530 [3298-3733] g). Maternal and umbilical cord blood samples were taken at delivery and a further blood sample of up to 2 mL was taken from the neonate at 3 weeks of age. A neonatal stool sample was collected at birth and also at 3 weeks of age (n=29). Sixteen out of 38 babies (42%) were exclusively breastfed for the duration of the study, while 9 babies received mixed feeding and 13 babies were exclusively formula-fed.

Flow cytometric analysis was used to assess the profile of major lymphocyte subsets in umbilical cord and neonatal blood samples at 3 weeks of age, as well as in adult blood samples. The proportion of CD3+ cells was lower in cord blood compared to maternal blood, while that of CD4+ cells was higher. CD8+ cell percentages were lower both at birth and at 3 weeks of age compared to maternal and non-pregnant adult samples (Figure 1a).

The proportion of CD4+ FoxP3+ CD25hi Tregs increased from 6.4% in cord blood to 8.0% within the first 3 weeks of life, comparable to the level in non-pregnant adults but remained lower than third trimester maternal samples (Figure 1b). Interestingly, within the different feeding groups at 3 weeks of age, the frequency of Tregs was nearly two-fold higher (9.3% vs 4.9%) in exclusively breastfed compared to exclusively formula-fed neonates (Figure 1c). We also examined the expression of selected cell surface markers on Treg cells at birth and at 3 weeks of age. HLA-DR expression increased during the first 3 weeks of life, potentially reflecting recent activation, however, no difference was detected in the expression of CD45RA, CD31 or CD69 between the two time points (Figure 1d). Of note, no difference was observed in the expression of these markers between the different feeding groups.

We then went on to determine the functional activity of T cells through analysis of intracellular cytokine and surface CD107a expression in response to mitogenic stimulation. The proportion of IL-8+ CD4+ cells was lower, whereas that of IFN- γ + CD4+ cells was higher in maternal compared to neonatal samples (Figure 2a). No differences were observed in the profile of IFN- γ , IL-4, IL-6 or IL-8 expression by CD4+ and CD8+ cells between birth and 3 weeks of age. However, the number of IL-17+ CD8+ cells, as well as the mean fluorescence intensity of IL-17 in CD4+ and CD8+ cells, increased during the first three weeks (Figure 3a and Supplementary Figure 1). Interestingly, at 3 weeks of age the mean fluorescence intensity of IFN- γ in CD4+ and CD8+ cells was higher in exclusively formula-fed neonates compared to those receiving breastmilk (Figure 3b). No further differences were observed between feeding groups.

A higher proportion of CD8+ cells expressed CD107a, a marker of cytotoxic degranulation, in non-pregnant adult samples compared to neonatal samples at birth and 3 weeks of age. The mean fluorescence intensity of CD107a expression on CD8+ cells was higher in adult compared to neonatal samples (Figures 2b and 3c). No differences were observed between feeding groups.

T cells of exclusively breastfed neonates show reduced proliferation in response to stimulation by maternal cells

We performed mixed lymphocyte reactions (MLRs) on blood samples of 37 mother-and-baby dyads. Initially, maternal cells were stimulated with irradiated cord or neonatal cells and here we observed increased proliferation of CD3+ and CD4+ cells in response to neonatal peripheral blood mononuclear cells (PBMCs) at 3 weeks of age compared to birth (Supplementary Figure 2a). A similar increase (CD3+: 5.4 vs 15.5% median proliferating cells, CD4+: 5.3 vs 18% median proliferating cells) was observed when responder T cells of a non-pregnant healthy adult were used in combination with neonatal stimulator cells (Supplementary Figure 2b).

We next utilized cord and neonatal T cells in MLRs against irradiated maternal PBMCs (Figure 4a). Interestingly, here we observed decreased proliferation in neonatal CD3+ and CD8+, but not CD4+ cells in response to maternal stimulator cells at 3 weeks of age compared to birth (Figure 4b).

We further examined the influence of neonatal nutrition on these proliferative responses at 3 weeks of age. Sixteen neonates had been exclusively breastfed whereas 13 had received only formula and 8 had undergone a mixed milk intake. The decrease in the proliferation rate of CD3+ cells was still evident in exclusively breastfed neonates (60.7 vs 28.9% median proliferating cells) but was not present in the mixed feeding and exclusively formula-fed groups (Figure 4c). The same pattern was observed in CD4+ and CD8+ cells. Interestingly, the proliferation rate of CD3+, CD4+ and CD8+ cells of exclusively breastfed neonates was comparable at birth and at 3 weeks of age when PBMCs of a non-pregnant healthy adult were used as stimulators ($n = 6$), reflecting that the neonatal tolerance is specific to maternal antigens.

Neonatal immune tolerance promoted by breastfeeding is mediated by regulatory T cells and is associated with a reduction in release of inflammatory cytokines

Having observed that breastfeeding promotes the expansion of Tregs and suppresses proliferative responses against maternal antigen, we next investigated if this immune tolerance was dependent on the presence of Tregs. To this end, we repeated the MLRs on a set of 6 mother-and-baby dyads where babies were

exclusively breastfed following the depletion of CD25+ cells (Figure 5a). Pregnancy is associated with peripheral accumulation of Tregs and the proliferation of maternal CD3+ cells in response to neonatal antigens increased both at birth (20.4 vs 59.7% median proliferating cells) and at 3 weeks of age (34.1 vs 57.1% median proliferating cells) following depletion of CD25+ cells (Figure 5b). The same pattern was observed for CD4+ but not in CD8+ cells. Of note, the proliferation of neonatal CD3+ cells in response to maternal antigens increased after depletion of CD25+ cells in samples taken at 3 weeks of age (71.4 vs 85.1% median proliferating cells) but this was not seen with the use of cord blood cells (Figure 5c). The same pattern was observed for CD4+ but not in CD8+ cells.

We also measured the concentration of cytokines in MLR supernatants ($n = 11$) produced by neonatal T cells of exclusively breastfed neonates in response to maternal antigens. The concentration of IFN- γ and TNF- α was found to be lower at 3 weeks of age compared to birth, whereas no difference was observed in case of the other cytokines tested (IL-4, IL-6, IL-8, IL-10, IL-17). The maximal IFN- γ and TNF- α producing capacity of neonatal T cells, tested by culturing with CD3/CD28 activator beads, was higher both at birth and at 3 weeks of age compared to the level seen in response to maternal antigens at 3 weeks (Figure 5d). As such, breastfeeding is seen to suppress the inflammatory Th1 cytokine response of neonatal T cells in response to maternal antigen stimulation.

Breastfeeding has modest impact on the gut microbiome in neonates born by caesarean section within the first 3 weeks of life

To evaluate the impact of breastfeeding on the neonatal gut microbiome, we analyzed stool samples from exclusively breastfed and exclusively formula-fed neonates collected at 3 weeks of age. Meconium samples had also been collected at birth but the amount of DNA extracted from these samples was consistently < 0.15 ng/ μ L. PCR amplification using 16S primers on these DNA samples yielded undetectable product for further analysis, reflecting minimal or no microbial colonization immediately after birth.

In the stool samples at 3 weeks of age, following microbial 16S rRNA gene amplification, a median frequency of 18,354 amplicon sequence variants (ASV) per sample were retained after trimming and filtering. The composition of gut microbiota from exclusively breastfed and exclusively formula-fed neonates was broadly similar and no differences in any alpha or beta diversity metrics were seen (Figure 6a). Principal component analysis (PCA) of gut microbiota composition of exclusively breastfed and exclusively formula-fed neonates demonstrated that individuals in these groups cluster closely together, and breastfeeding is associated with the presence of *Gemella* (Figure 6b). Linear discriminant analysis (LDA) effect size (LEfSe) revealed enrichment of the *Veillonella* and *Gemella* taxa in exclusively breastfed neonates (Figure 6c). Random Forest (RF) analysis identified the presence of *Staphylococcus*, followed by that of *Gemella* to be the most significant parameters distinguishing the two groups of exclusively breastfed and exclusively formula-fed neonates (Figure 6d).

Network modelling links *Veillonella* to regulatory T cell expansion whilst skin-associated bacteria enhance T cell proliferation in breastfed neonates

Finally, we undertook an integrative analysis of the combined data from flow cytometry, MLR and microbiome sequencing of neonates at 3 weeks of age. Network modelling revealed a range of positive and negative correlations between these parameters. In breastfed neonates CD4+ and CD8+ proliferative responses against maternal antigen were strongly correlated with *Gemella* and skin-associated taxa (Figure 7a). The presence of *Veillonella* within the microbiome correlated with the prevalence of Tregs at 3 weeks and this effect was independent of nutrition history (Figure 7b). In breastfed neonates *Veillonella* was also associated with HLA-DR expression on CD4+ cells and IFN- γ production in CD8+ cells. These findings suggest that *Veillonella* may act to enhance regulatory responses in the early period of life whereas skin-associated bacteria, potentially acquired through breastfeeding, may act to promote proliferative responses.

DISCUSSION

The influence of early life nutrition on the development of the immune response has not previously been

studied in the first few weeks of life. This is an important question as epidemiological data suggest that breastfeeding is associated with long-term health benefits, such as a lower incidence of allergy, asthma, diabetes, celiac disease and multiple sclerosis¹⁹⁻²². This mechanism may be imprinted early after birth when the immune system faces the dual challenge of establishing inflammatory capacity against pathogens whilst developing tolerance towards harmless antigens.

A striking finding was that Tregs expand substantially in the first 3 weeks of life and this expansion was more profound in breastfed babies in contrast to those receiving formula feed. Tregs of breastfed neonates also display an activated phenotype with increased expression of HLA-DR, a marker of increased suppressive activity²³. On the other hand, changes in the profile of pro-inflammatory cytokine production were also observed at this early stage of life. IL-8 production, a major phenotypic attribute within cord blood, was largely maintained but a striking feature was the increase in intensity of IL-17 production by both CD4+ and CD8+ cells by 3 weeks of age. This is likely to reflect recognition of bacterial antigen during establishment of the microbiome and may be balanced by the coordinated Treg expansion during this period. An increase in serum IL-17 has been shown at 4 weeks and is likely explained by these observations⁵. Most of these features were independent of nutrition although IFN- γ production by T cells was lower in exclusively breastfed neonates. Our observation that CD8+ cells are less abundant and have reduced cytotoxic capacity in neonates compared to adults confirms previous results^{24,25}.

One of the most interesting findings was that T cells from breastfed neonates display reduced proliferative responses and produce substantially lower levels of Th1 cytokines when challenged with maternal cells. This was specific to maternal antigens and was not present against unrelated PBMC and did not result from an intrinsic reduction of cytokine producing capacity. As such this reflects the development of immunological tolerance against non-inherited maternal antigens (NIMA) in exclusively breastfed neonates. Importantly, we were also able to show that NIMA-specific tolerance was mediated by Tregs, and is therefore linked to the expansion of this population in breastfed neonates.

An additional observation was that neonatal PBMC at 3 weeks of age triggered stronger immune responses from maternal PBMC compared to cord blood cells. This may reflect maturation of antigen presentation function by 3 weeks of age, although this was not assessed in this study. This also indicates that the fetal immune system may contribute to suppression of maternal immune recognition during pregnancy by maintaining a tolerogenic phenotype prior to parturition.

It is interesting to speculate on potential mechanisms by which breastfeeding can promote NIMA-specific tolerance in neonates. Our observations likely reflect immune tolerance to gastrointestinal presentation of maternal cells within breastmilk²⁶. Transplacental passage of cells during pregnancy leads to reciprocal microchimerism that can persist for many years. Furthermore, this 'microchimerism' of maternal cells supports fertility in female offspring by promoting immune tolerance to NIMA during next-generation pregnancies²⁷. Beneficial effects are also seen when NIMA are shared between donors and recipients of allogeneic renal or hemopoietic stem cell transplantation. Importantly, the establishment of NIMA-specific tolerance has been shown to be dependent on breastfeeding and nutritional history is also a determinant of NIMA-associated transplant outcome^{28,29}. Our findings show that breastfeeding directly promotes the development of Tregs that suppress recognition of maternal tissue, thus likely supporting maternal microchimerism and potentially conferring lifelong benefits in relation to fertility and immune protection against infectious agents and cancer^{27,30}.

A further recent observation is that breastfeeding, through the transfer of human milk oligosaccharides, exerts important prebiotic and immunomodulatory effects including the development of tolerogenic dendritic cells which prime Tregs^{31,32}.

We were also interested to assess how nutrition could impact on the formation of the early microbiome and how this might correlate with immune function. Microbial composition was broadly comparable in breastfed and formula-fed neonates and this is likely to reflect the fact that all babies in our cohort were delivered by caesarean section. Dysbiosis of the microbiota has been found to occur following delivery by caesarean section

and in infants who are not breastfed^{33,34}. Nevertheless, although it may take several months for nutrition to markedly influence microbiome composition³⁵ subtle differences in microbial diversity were already apparent at 3 weeks of life. In line with previously published results³⁶, we observed that the gut microbiome of breastfed neonates is more abundant in short chain fatty acid (SCFA) producing bacterial genera, such as *Gemella* and *Veillonella*. SCFAs, in particular propionate and butyrate, play an important role in promoting Treg differentiation and proliferation via the inhibition of histone deacetylases¹¹. This notion is supported by a link between the presence of *Veillonella* and the proportion of Tregs at 3 weeks of age in our network modelling analysis.

We selected elective caesarean deliveries for our study as labor is known to promote pro-inflammatory changes³⁷. Further studies will therefore be needed to establish the relative contribution of mode of delivery and nutritional history on the development of NIMA-specific tolerance in the neonate. A further limitation of this work is the relatively low number of neonates in the examined feeding groups. Nevertheless, we established a unique and homogenous cohort of healthy neonates who were sampled at 3 weeks of age exclusively for the purposes of this study.

In summary, we demonstrate that the neonatal immune system undergoes substantial maturation in the first 3 weeks of life with an increase in IL-17 production in T cells and a balanced increase in the Treg population. Moreover, breastfed neonates show a specific and Treg dependent reduction in proliferative T cell responses to NIMA, associated with a reduction in inflammatory cytokine production. These findings add to our understanding of mechanisms by which early life nutrition can determine long term health outcomes³⁸.

Data availability

The datasets generated and analyzed during the current study are available from the corresponding author on request. Microbiome sequencing data were deposited in the SRA database (accession number PR-JNA629085).

References

- 1 Shane AL, Sánchez PJ, Stoll BJ. Neonatal sepsis. *Lancet* 2017;390:1770-80.
- 2 Hug L, Alexander M, You D, et al. National, regional, and global levels and trends in neonatal mortality between 1990 and 2017, with scenario-based projections to 2030: a systematic analysis. *Lancet Glob Health* 2019;7: e710-20.
- 3 Fleischmann-Struzek C, Goldfarb DM, Schlattmann P, et al. The global burden of paediatric and neonatal sepsis: a systematic review. *Lancet Respir Med* 2018;6:223-30.
- 4 Zhang X, Zhivaki D, Lo-Man R. Unique aspects of the perinatal immune system. *Nat Rev Immunol* 2017;17:495-507.
- 5 Olin A, Henckel E, Chen Y, et al. Stereotypic immune system development in newborn children. *Cell* 2018;174:1277-92.
- 6 Lee AH, Shannon CP, Amenogbe N, et al. Dynamic molecular changes during the first week of human life follow a robust developmental trajectory. *Nat Commun* 2019;10:1092.
- 7 Aluvihare VR, Kallikourdis M, Betz AG. Regulatory T cells mediate maternal tolerance to the fetus. *Nat Immunol* 2014;5:266-71.
- 8 Kollmann TR, Kampmann B, Mazmanian SK, et al. Protecting the newborn and young infant from infectious diseases: lessons from immune ontogeny. *Immunity* 2017;46:350-63.
- 9 Mold JE, Michaelsson J, Burt TD, et al. Maternal alloantigens promote the development of tolerogenic fetal regulatory T cells in utero. *Science* 2008;322:1562-5.
- 10 McGovern N, Shin A, Low G, et al. Human fetal dendritic cells promote prenatal T-cell immune suppression through arginase-2. *Nature* 2017;546:662-6.

- 11 Arpaia N, Campbell C, Fan X, et al. Metabolites produced by commensal bacteria promote peripheral regulatory T-cell generation. *Nature* 2013;504:451-455.
- 12 Salminen S, Gibson GR, McCartney AL, et al. Influence of mode of delivery on gut microbiota composition in seven year old children. *Gut* 2004;53:1388-9.
- 13 Gritz EC, Bhandari V. The human neonatal gut microbiome: a brief review. *Front Pediatr* 2017;3:17.
- 14 Witkowska-Zimny M, Kaminska-El-Hassan E. Cells of human breast milk. *Cell Mol Biol Lett* 2017;22:11.
- 15 Caporaso JG, Lauber CL, Walters WA, et al. Ultra-high-throughput microbial community analysis on the Illumina HiSeq and MiSeq platforms. *ISME J* 2012;6:1621-4.
- 16 Quraishi MN, Acharjee A, Beggs AD, et al. A pilot integrative analysis of colonic gene expression, gut microbiota and immune infiltration in primary sclerosing cholangitis-inflammatory bowel disease: association of disease with bile acid pathways. *J Crohns Colitis* 2020;14:935-47.
- 17 Hall M, Beiko RG. 16S rRNA gene analysis with QIIME2. *Methods Mol Biol* 2018;1849:113-29.
- 18 Breiman L. Random Forests. *Machine Learning* 2001;45:5-32.
- 19 Vieira Borba V, Sharif K, Shoenfeld Y. Breastfeeding and autoimmunity: Programing health from the beginning. *Am J Reprod Immunol* 2018;79:e12778.
- 20 Oddy, W. H. Breastfeeding, childhood asthma, and allergic disease. *Ann Nutr Metab* 2017;70 Suppl 2:26-36.
- 21 Mathias JG, Zhang H, Soto-Ramirez N, et al. The association of infant feeding patterns with food allergy symptoms and food allergy in early childhood. *Int Breastfeed J* 2019;14:43.
- 22 Kull I, Wickman M, Lilja G, et al. Breast feeding and allergic diseases in infants-a prospective birth cohort study. *Arch Dis Child* 2002;87:478-81.
- 23 Schaier M, Seissler M, Schmitt E, et al. DR(high+)CD45RA(-)-Tregs potentially affect the suppressive activity of the total Treg pool in renal transplant patients. *PLoS One* 2012;7:e34208.
- 24 Fike AJ, Kumova OK, Carey AJ. Dissecting the defects in the neonatal CD8+ T-cell response. *J Leukoc Biol* 2019;106:1051-61.
- 25 Galindo-Albarrán AO, López-Portales OH, Gutiérrez-Reyna DY, et al. CD8+ T cells from human neonates are biased toward an innate immune response. *Cell Rep* 2016;17:2151-60.
- 26 Moles JP, Tuaillon E, Kankasa C, et al. Breastmilk cell trafficking induces microchimerism-mediated immune system maturation in the infant. *Pediatr Allergy Immunol* 2018;29:133-43.
- 27 Kinder JM, Stelzer IA, Arck PC, et al. Immunological implications of pregnancy-induced microchimerism. *Nat Rev Immunol* 2017;17:483-94.
- 28 Aoyama K, Matsuoka KI, Teshima T. Breast milk and transplantation tolerance. *Chimerism* 2010;1:19-20.
- 29 Aoyama K, Koyama M, Matsuoka K, et al. Improved outcome of allogeneic bone marrow transplantation due to breastfeeding-induced tolerance to maternal antigens. *Blood* 2009;113:1829-33.
- 30 Darby MG, Chetty A, Mrjden D, et al. Pre-conception maternal helminth infection transfers via nursing long-lasting cellular immunity against helminths to offspring. *Sci Adv* 2019;5:eaav3058.
- 31 Xiao L, Van't Land B, Engen PA, et al. Human milk oligosaccharides protect against the development of autoimmune diabetes in NOD-mice. *Sci Rep* 2018;8:3829.
- 32 Xiao L, van De Worp W, Stassen R, et al. Human milk oligosaccharides promote immune tolerance via direct interactions with human dendritic cells. *Eur J Immunol* 2019;49:1001-14.

- 33 Logan AC, Jacka FN, Prescott SL. Immune-microbiota interactions: dysbiosis as a global health issue. *Curr Allergy Asthma Rep* 2016;16:13.
- 34 Shao Y, Forster SC, Tsaliki E, et al. Stunted microbiota and opportunistic pathogen colonization in caesarean-section birth. *Nature* 2019;574:117-21.
- 35 Davis EC, Wang M, Donovan SM. The role of early life nutrition in the establishment of gastrointestinal microbial composition and function. *Gut Microbes* 2017;8:143-71.
- 36 Timmerman HM, Rutten NBMM, Boekhorst J, et al. Intestinal colonisation patterns in breastfed and formula-fed infants during the first 12 weeks of life reveal sequential microbiota signatures. *Sci Rep* 2017;7:8327.
- 37 Norman JE, Bollapragada S, Yuan M, et al. Inflammatory pathways in the mechanism of parturition. *BMC Pregnancy Childbirth* 2007;7 Suppl 1:S7.
- 38 Binns C, Lee M, Low WY. The long-term public health benefits of breastfeeding. *Asia Pac J Public Health* 2016;28:7-14.

Figure legends

Figure 1. Alterations of T cell subsets and the regulatory T cell (Treg) phenotype in neonates between birth and 3 weeks of age. **a**, The frequency of CD3+, CD4+ and CD8+ cells in neonatal blood samples (n = 17) at birth and at 3 weeks of age, as well as in maternal blood (n = 17) and healthy controls (n = 8). **b**, The frequency of CD4+ FoxP3+ CD25hi cells in neonatal blood samples (n = 19) at birth and at 3 weeks of age, as well as in maternal blood (n = 19) and healthy controls (n = 13). **c**, The frequency of CD4+ FoxP3+ CD25hi cells in neonatal blood samples at 3 weeks of age grouped according to the feeding method: exclusively breastfed (n = 9), mixed feeding (n = 5) and formula-fed (n = 5) neonates. **d**, The expression of selected cell surface markers on Tregs in neonatal blood samples at birth and at 3 weeks of age (n = 19). Horizontal lines represent medians and interquartile ranges. * p < 0.05, ** p < 0.01, *** p < 0.001

Figure 2. Representative dot-plots of intracellular cytokine and cell surface cytotoxic markers following mitogenic stimulation in a neonatal blood sample at birth and at 3 weeks of age as well as in a maternal blood sample. **a**, Intracellular cytokines were gated within CD4+ cells. **b**, Cell surface expression of CD107a, a marker of cytotoxic degranulation and the intracellular expression of IFN- γ are shown within CD8+ cells.

Figure 3. Alterations of the pro-inflammatory and cytotoxic immunophenotype in neonates between birth and 3 weeks of age. **a**, The intracellular frequency and mean fluorescence intensity (MFI) of selected pro-inflammatory cytokines in CD4+ cells in neonatal blood samples at birth and at 3 weeks of age (n = 17). **b**, The intracellular frequency and MFI of interferon gamma (IFN- γ) in CD4+ cells in neonatal blood samples at 3 weeks of age grouped according to the feeding method: exclusively breastfed (n = 8), mixed feeding (n = 5) and formula-fed (n = 4) neonates. **c**, The frequency of CD8+ and CD8+ CD107a+ cells and MFI of CD107a in CD8+ cells in neonatal blood samples (n = 17) at birth and at 3 weeks of age, as well as in maternal blood samples (n = 17) and healthy controls (n = 8). Horizontal lines represent medians and interquartile ranges. * p < 0.05, ** p < 0.01, *** p < 0.001

Figure 4. Neonatal T cell response upon maternal antigen stimulation. **a**, Representative sample of a mixed lymphocyte reaction (MLR) at birth and at 3 weeks of age with negative and positive controls. Positive controls were established with the addition of CD3/CD28 activator beads instead of stimulator cells. Negative controls were established in enriched media only. Samples were incubated for 5 days. **b**, Percentage of neonatal proliferating T cells (n = 37) at birth and at 3 weeks of age in response to maternal irradiated cells in the CD3+, CD4+ and CD8+ cell subsets. **c**, Percentage of neonatal proliferating CD3+ cells at birth and at 3 weeks of age in response to maternal irradiated cells grouped according to the feeding method: exclusively breastfed (n = 16), mixed feeding (n = 8) and formula-fed (n = 13) neonates. Horizontal lines represent medians and interquartile ranges. * p < 0.05, ** p < 0.01

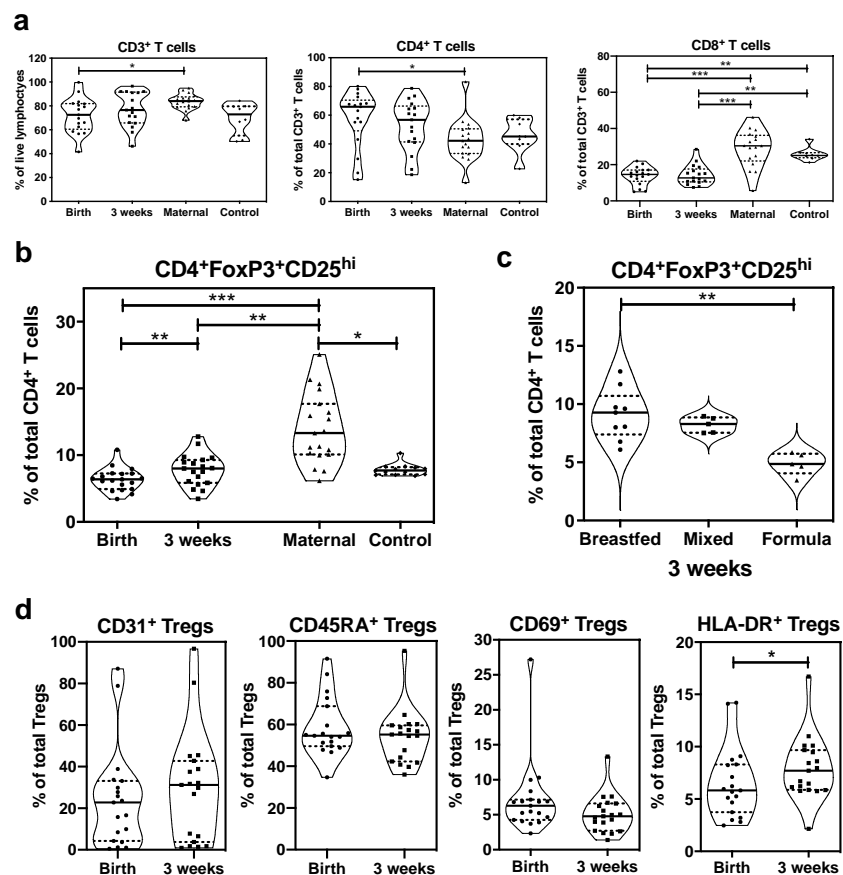
Figure 5. Maternal and neonatal T cell response in mixed lymphocyte reactions (MLR) following the depletion of CD25+ cells and pro-inflammatory cytokine production by neonatal T cells in exclusively breastfed neonates in MLR upon maternal antigen stimulation at birth and at 3 weeks of age. **a**, Representative dot-plots with and without the depletion of CD25+ cells in a neonatal sample at 3 weeks of age, gated within CD3+ cells. CD25+ cells were depleted using magnetic microbead separation. **b**, Percentage of maternal proliferating T cells ($n = 6$) in response to neonatal stimulator cells of exclusively breastfed neonates from birth and 3 weeks of age in the CD3+ subset. **c**, Percentage of neonatal proliferating T cells ($n = 6$) in response to maternal stimulator cells at birth and at 3 weeks of age in the CD3+ subset of exclusively breastfed neonates. **d**, The concentration of IFN- γ and TNF- α was found to be lower at 3 weeks of age compared to birth ($n = 11$). The maximal IFN- γ and TNF- α producing capacity of neonatal T cells was also assessed at birth and at 3 weeks of age by culturing them with CD3/CD28 activator beads. The production of IFN- γ and TNF- α was higher both at birth and at 3 weeks of age compared to the level seen in response to maternal antigens at 3 weeks. Horizontal lines represent medians and interquartile ranges. * $p < 0.05$, ** $p < 0.01$, *** $p < 0.001$

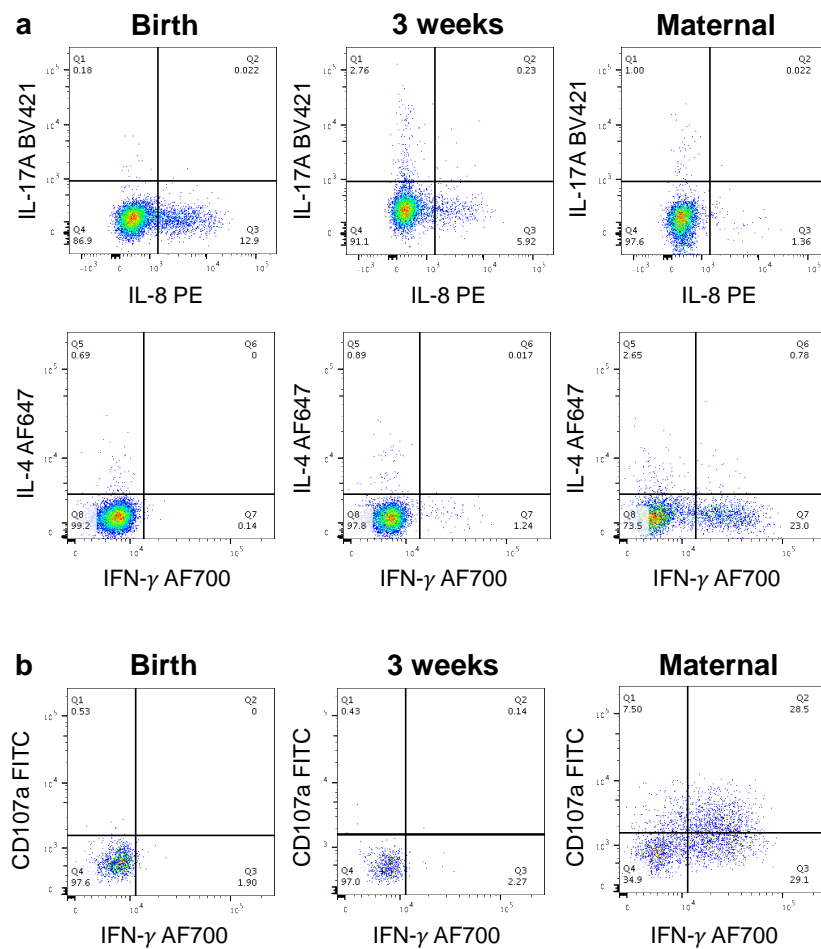
Figure 6. Microbiome analysis of neonatal stool samples at 3 weeks of age in exclusively breastfed ($n = 9$) and exclusively formula-fed ($n = 12$) neonates. **a**, Relative frequency of bacterial phyla in the two cohorts. **b**, Principal component analysis (PCA) of gut microbiota composition of exclusively breastfed (red) and exclusively formula-fed (blue) neonates at 3 weeks of age determined by bacterial 16S rRNA amplification. Numbers represent the individual study number of each participant. Pooled variables of milk received are represented by the large red circle for breastmilk and the large blue triangle for formula, respectively. **c**, Association of specific microbial taxa with the feeding method by linear discriminant analysis (LDA) effect size (LEfSe). Red indicates taxa enriched in exclusively breastfed neonates. **d**, Ranking of gut microbial strains using the Random Forest (RF) method in exclusively breastfed (BM) and exclusively formula-fed neonates at 3 weeks of age.

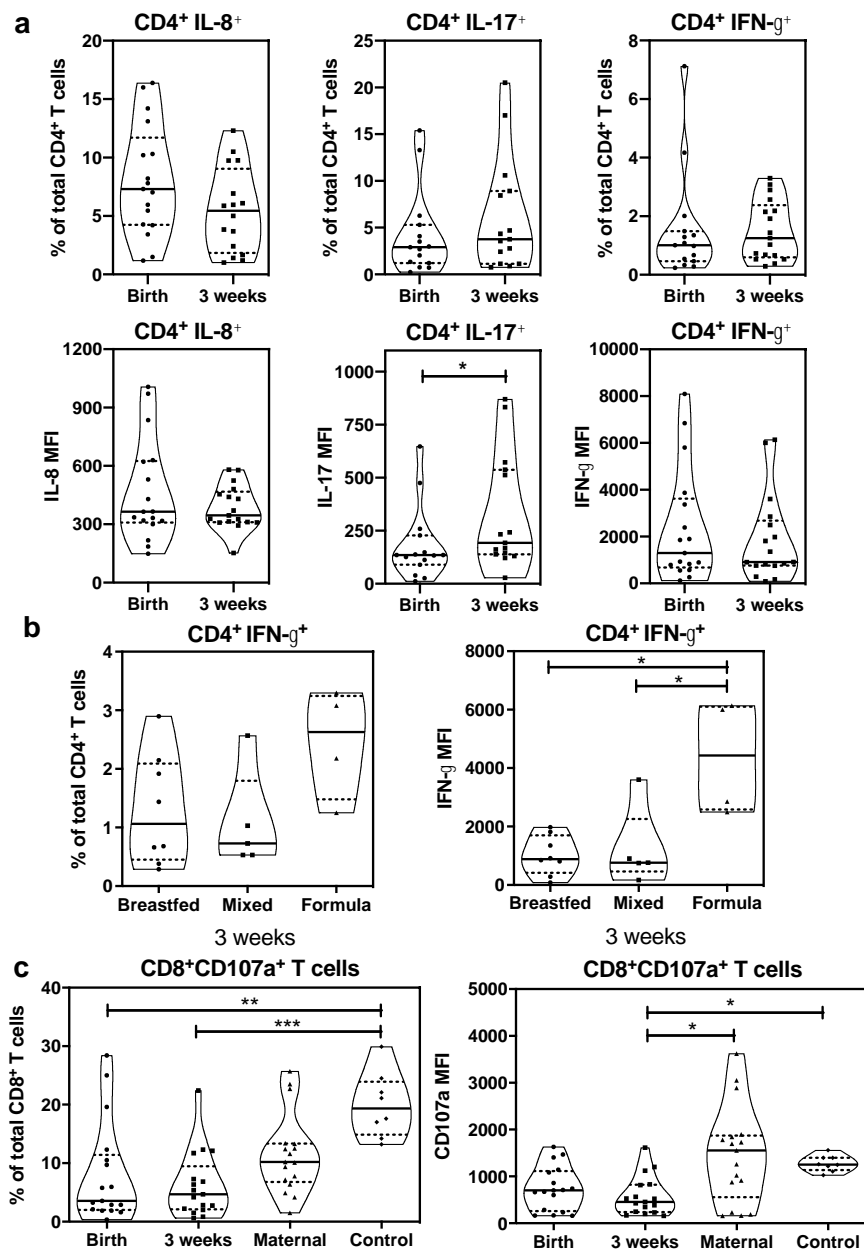
Figure 7. Integrated analysis of mixed lymphocyte reaction (MLR), flow cytometry and microbiome data of **a**, exclusively breastfed ($n = 9$) and **b**, exclusively formula-fed ($n = 5$) neonates at 3 weeks of age. Various positive and negative correlations between the studied parameters were revealed. Green represents a positive correlation, whereas red represents a negative correlation. Thicker lines represent stronger correlations. Nodes in blue represent MLR data, nodes in black represent microbiome data, and nodes in purple and orange represent flow cytometry data from the panels with and without mitogenic stimulation, respectively.

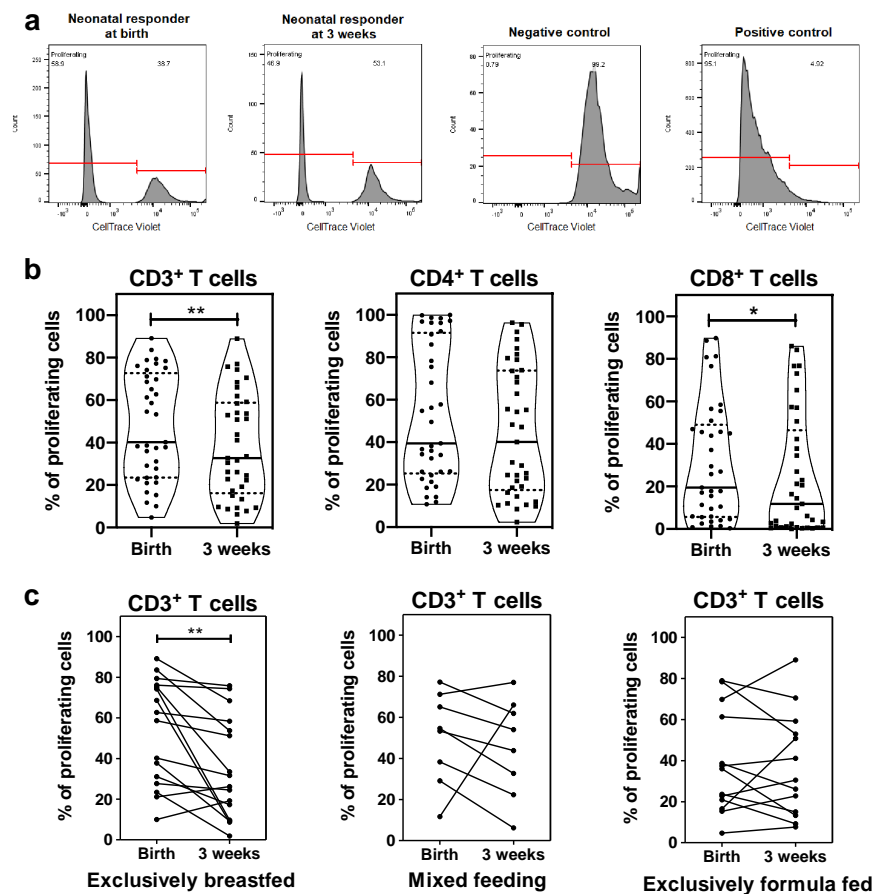
Supplementary Figure 1. The intracellular frequency and mean fluorescence intensity (MFI) of selected pro-inflammatory cytokines in CD8+ cells in neonatal blood samples at birth and at 3 weeks of age ($n = 17$). Horizontal lines represent medians and interquartile ranges. * $p < 0.05$

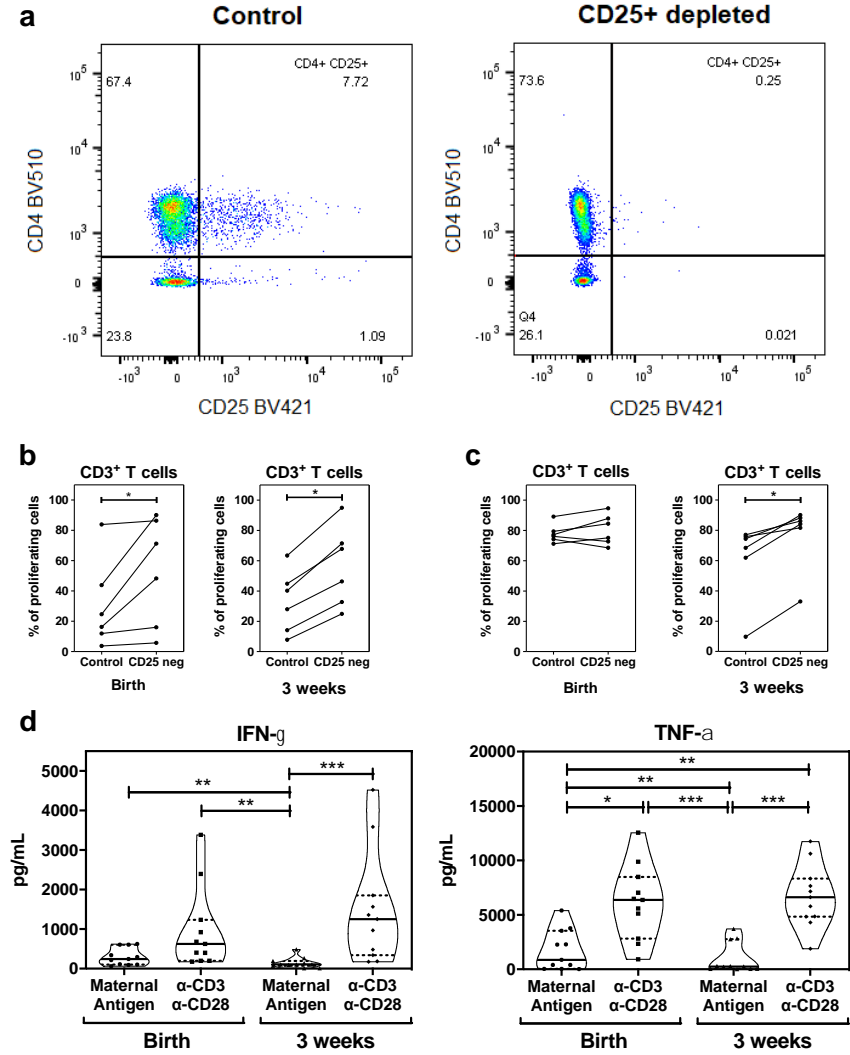
Supplementary Figure 2. Maternal T cell response upon neonatal antigen stimulation from birth and 3 weeks of age. **a**, Percentage of maternal proliferating T cells ($n = 37$) in the CD3+, CD4+ and CD8+ cell subsets in response to neonatal irradiated cells. **b**, Percentage of proliferating T cells of a third-party, non-pregnant control individual ($n = 6$) in the CD3+, CD4+ and CD8+ cell subsets in response to neonatal irradiated cells. Horizontal lines represent medians and interquartile ranges. * $p < 0.05$

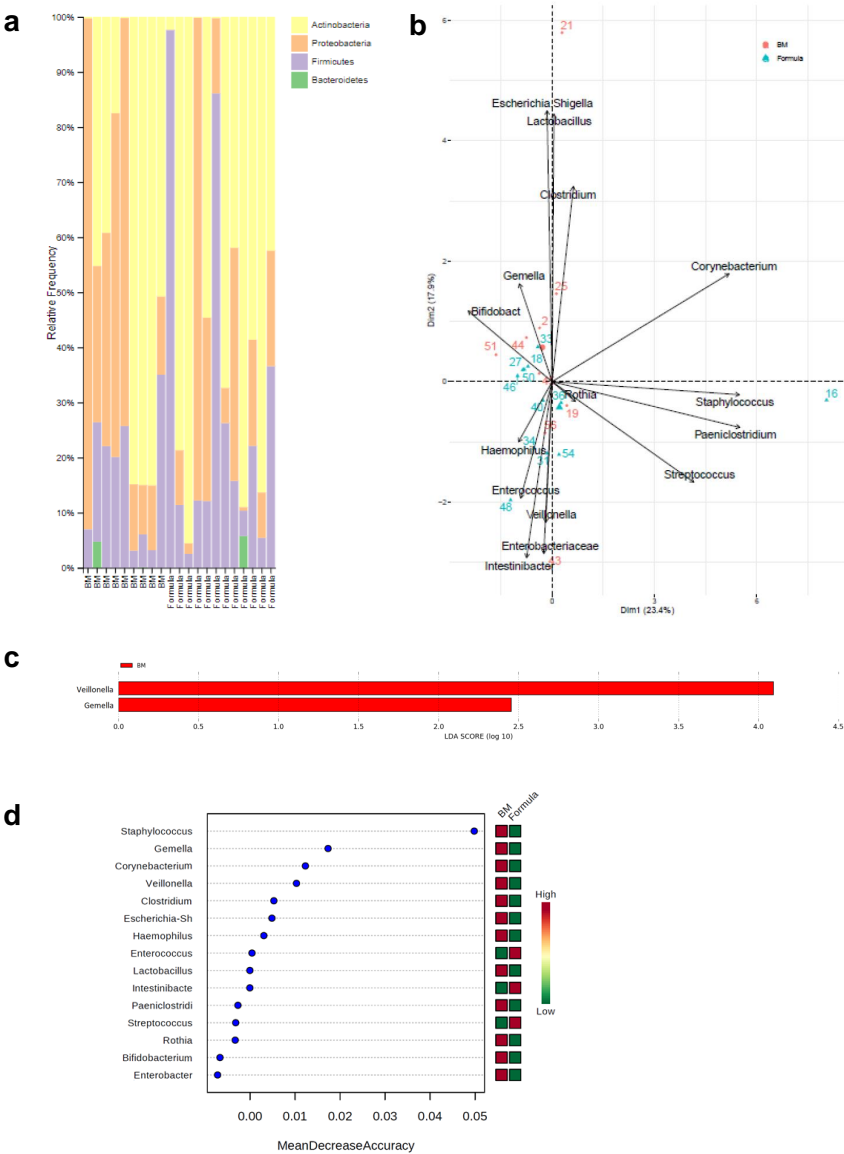




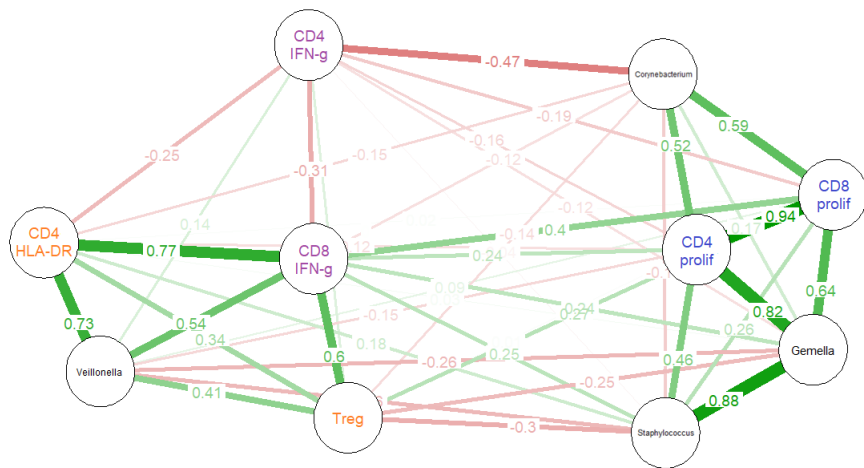








a Breastfeeding



b **Formula feeding**

